Theoretical and Applied Climatology
https://doi.org/10.1007/s00704-020-03483-y

ORIGINAL PAPER

Present-day climate and projected future temperature and precipitation changes in Ecuador

Oscar Chimborazo [1,2] · Mathias Vuille [1]

Received: 8 May 2020 / Accepted: 23 November 2020

Abstract

Ecuador is likely to experience significant impacts associated with future changes in climate, but future projections for this region are challenging due to the complex topography and a wide range of climatic conditions. Here we use the Weather Research and Forecasting (WRF) model run at 10 km horizontal resolution over a domain encompassing all of Ecuador to investigate future changes in temperature and precipitation for the middle of the twenty-first century (2041–2070) under a low (RCP4.5) and a high (RCP8.5) emission scenario. The model was validated by running 30-year control runs for the present climate, driven both by the Climate Forecast System Reanalysis (CFSR) and the CCSM4 General Circulation Model. Bias and different correlation coefficient metrics were employed to compare the present-day model results with gridded (CRU TS v 4.03 and CHIRPS v 2.0) and in situ meteorological observations. Detailed hydrometeorological analyses over the Andes in both space and time domains show that WRF accurately simulates temperature variability. The precipitation seasonal cycle and interannual variability are also adequately simulated, but the model shows a general dry bias over the lowlands and a significant wet bias along the eastern Andean slopes. Results from future projections show that Ecuador could warm by an additional 1–2 K by the middle of the century compared with the end of the twentieth century. This warming is highly elevation-dependent, subjecting the highest peaks of the Andes to the strongest future warming. Bias-corrected future precipitation changes document a drying trend along coastal areas in RCP4.5 and increased future precipitation along the eastern Andean slopes in both scenarios.

1 Introduction

Ecuador is characterized by a complex climate, resulting from a combination of factors, which include the Andean topography, the interactions of Hadley and Walker circulations near the equator (Hastenrath and Lamb 2004), the constantly high solar radiation receipts at near-equator latitudes, and the influence of climate modes associated with Pacific and Atlantic sea surface temperature anomalies, including—but not limited to—the El Niño–Southern Oscillation (ENSO) phenomenon (Vuille et al. 2000; Francou et al. 2004; Recalde-Coronel et al. 2014; Morán-Tejeda et al. 2016; Vicente-Serrano et al. 2017; Quishpe-Vásquez et al. 2019). The multiple interactions between these different systems in both space and time lead to one of the most diverse sets of climates over a fairly limited domain that encompasses Ecuador. The continuous barrier formed by the Andes further interacts with and modulates the atmospheric circulation, producing synoptic and mesoscale phenomena, which generate contrasting climates along the Andean slopes and the inter-Andean valleys (Mora and Willems 2012; Tobar and Wyseure 2018.).

The climate in Ecuador, however, is rapidly changing due to anthropogenic forcing associated with the increasing concentration of greenhouse gases in our atmosphere, as manifested by increasing temperature, changing rainfall patterns, glacier retreat, and ecosystem changes (Francou et al. 2004; Buytaert et al. 2011; Jacobsen et al. 2012; Rabatel et al. 2013; Michelutti et al. 2015; Morueta-Holme et al. 2015; Vuille et al. 2015, 2018; Morán-Tejeda et al. 2016; Tobar and Wyseure 2018). Assessing how such changes in radiative forcing will manifest themselves on local to regional scales over a region such as Ecuador, which is influenced by so many climatic factors, is thus a massive challenge. Data produced within the framework of the Intergovernmental Panel

✉ Mathias Vuille
mvuille@albany.edu

[1] Department of Atmospheric and Environmental Sciences, University at Albany, State University of New York, 1400 Washington Avenue, Albany, NY 12222, USA

[2] Dirección de Investigación y Desarrollo, Facultad de Ingeniería Civil y Mecánica, Universidad Técnica de Ambato, Av. Los Chasquis y Río Payamino, 180206 Ambato, Ecuador

Published online: 08 January 2021

on Climate Change (IPCC) by the Coupled Model Intercomparison Project Phases 5 (CMIP5) and 6 (CMIP6) are not sufficiently resolved, neither horizontally nor vertically, to reproduce key aspects of Ecuadorian climate, especially as it relates to topographically forced phenomena (e.g., the elevation-dependent warming; Pepin et al. 2015), in particular at a local scale and over topographically complex regions such as the Andes. Therefore, it is necessary to downscale the information provided by GCMs to obtain higher-resolution projections of climate scenarios for studies at regional scales.

Some studies of climate and climate change over Ecuador relied on GCMs (e.g., Buytaert et al. 2009; Campozano et al. 2017), while others employed Regional Climate Models (RCMs) to study aspects of climate or climate change over Ecuador (e.g., Urrutia and Vuille 2009; Buytaert et al. 2010; Ochoa et al. 2016; Heredia et al. 2018; Campozano et al. 2020). Urrutia and Vuille (2009) developed regional climate change projections over the tropical Andes using an RCM, the PRECIS model, over a domain that included Ecuador, while McGlone and Vuille (2012) used the same RCM to study the influence of varying boundary conditions on the simulations. Buytaert et al. (2010) also analyzed the PRECIS performance by focusing on precipitation over the Ecuadorian Andes, with mixed results.

The main objective of this study is to assess the capabilities of a different RCM, the Weather and Research Forecast (WRF) model (Skamarock et al. 2008), commonly used in weather and climate research, to adequately simulate the present-day climate of Ecuador, with a special emphasis on the Andean region. An additional goal is to investigate how precipitation and temperature might change in different regions of Ecuador by the middle of this century under two different emissions scenarios, giving special attention to future differential warming as a function of elevation in the Andes.

To achieve this goal, we conducted a series of simulations with WRF for both present day and the mid twenty-first century (2041–2070). We chose WRF because it is an open-source software, which makes it easily configurable for different case studies (e.g., Rasmussen et al. 2011; Rasmussen et al. 2014; Letcher and Minder 2017; Minder et al. 2018). The use of WRF is also appealing because it has already been used widely over South America to analyze atmospheric dynamics and in particular precipitation processes. Solman and Blasquez (2019), for example, recently documented that the WRF model systematically adds value to the simulation of South American precipitation when compared with the driving GCM, performing the best out of the all RCM's analyzed within the CORDEX-SA framework.

Several studies have also investigated the performance of WRF over the Andes, including its sensitivity to model resolution, domain choice, and how well it simulates mountain circulation and orographic precipitation processes (e.g., Moya-Alvarez et al. 2019). Most of these studies concluded that the performance of WRF over complex terrain tends to improve with increasing resolution and when aggregated over longer, monthly time scales, but that in general precipitation along the Andes is overestimated by WRF (Ochoa et al. 2016; Mourre et al. 2016; Junquas et al. 2018; Saavedra et al. 2020), although some studies also came to opposite conclusions (Heredia et al. 2018). Other studies investigated how WRF improves on the driving boundary conditions over the Andes (Ochoa et al. 2016; Posada-Marin et al. 2019) and how well WRF can simulate teleconnections between precipitation over the Andes and remote sea surface temperature (SST) fields (Martinez et al. 2019). Most recently, WRF was also employed to assess future drought projections for Ecuador based on three different CMIP5 models (Campozano et al. 2020).

To our knowledge, however, no studies exist, which have assessed the capability of the WRF model to reproduce observed climate variability at high resolution over all of Ecuador when driven with the CESM (CCSM) General Circulation model and with CSFR reanalysis data, one of the most commonly employed reanalysis-WRF combinations (e.g., Meyer and Jin 2016; Norris et al. 2019; Toride et al. 2019). Similarly, no studies have assessed future trends in temperature at high elevation in the Andes at sufficient spatial resolution to resolve specific elevation-dependent feedbacks that could lead to elevation-dependent warming, even though WRF is well suited for this task (e.g., Letcher and Minder 2017; Minder et al. 2018).

Here we present the results from four 30-year simulations over the domain of continental Ecuador. Two simulations correspond to the downscaling of historical and present-day climate spanning the late twentieth century and are forced with a GCM (CCSM4) and reanalysis data (CSFR), respectively. We validate these two simulations with several station-based and gridded observational data sets to highlight the potential and limitations of these high-resolution simulations to represent the present-day climate in Ecuador. When analyzing the results from these simulations, more weight was given to the results over the Andes region, as it has the most complex topography, thereby representing a major challenge for climate models, but also because elevation-dependent warming (EDW; Pepin et al. 2015) in the Andes is an area of major concern (Vuille and Bradley 2000; Vuille et al. 2015). Finally, we conducted two WRF experiments to simulate future climatic conditions, spanning the period 2041–2070, again driven by CCSM4 and following the Representative Concentration Pathway (RCP) 4.5 and 8.5 scenarios, respectively (van Vuuren et al. 2011). We analyze the resulting projected future changes in mean temperature and precipitation for different seasons and apply a bias correction, based on the prior model validation. Finally, we investigate the elevation-dependent warming (EDW) for both eastern and western Andean slopes under both medium (RCP4.5) and high emission (RCP8.5) scenarios.

2 Methods and data

2.1 WRF model setup

Here, we used the Advanced Research WRF (ARW) version 3.7.1 (Wang et al. 2016) as an RCM that covers entire Ecuador with a horizontal grid resolution of 10 km and 51 vertical levels from surface to 10 hPa. We perform model runs forced by both the Community Climate System Model version 4 (CCSM4; Gent et al. 2011) and with the Climate Forecast System Reanalysis (CFSR; Saha et al. 2010a,b) to asses differences in the performance of WRF when driven with a GCM versus reanalysis data.

The model domain of our simulations is shown in Fig. 1. In this study, we refer to the simulation domain and the study domain. The former is the region described by the geographical limits in the configuration file of the WRF model, and the latter is a smaller subset region of the simulation domain. The study domain is smaller than the simulation domain as lateral boundary effects that might arise in the simulation have to be taken into account. Performing the reanalysis-forced simulations only required a single domain to achieve the downscaled target resolution of 10 km, since both experiments used CFSR as boundary conditions, which already has a fairly high resolution of 50 km. On the other hand, a two-step downscaling process was needed for the GCM-forced simulations, because the resolution of the GCM is about 1° (~ 111 km). Therefore, for the GCM downscaling experiments, a parent domain of 50 km resolution and a nested domain of 10 km resolution were set. Figure 1 shows the configuration of these three domains.

Since different combinations of the available parameterizations in WRF will produce different results, and running an ensemble of different model configurations is not practical, Chimborazo (2018) performed a series of sensitivity tests to assess which combination of parameterizations best represents temperature and precipitation variability over the Ecuadorian territory. Based on these results, we implemented the NCAR

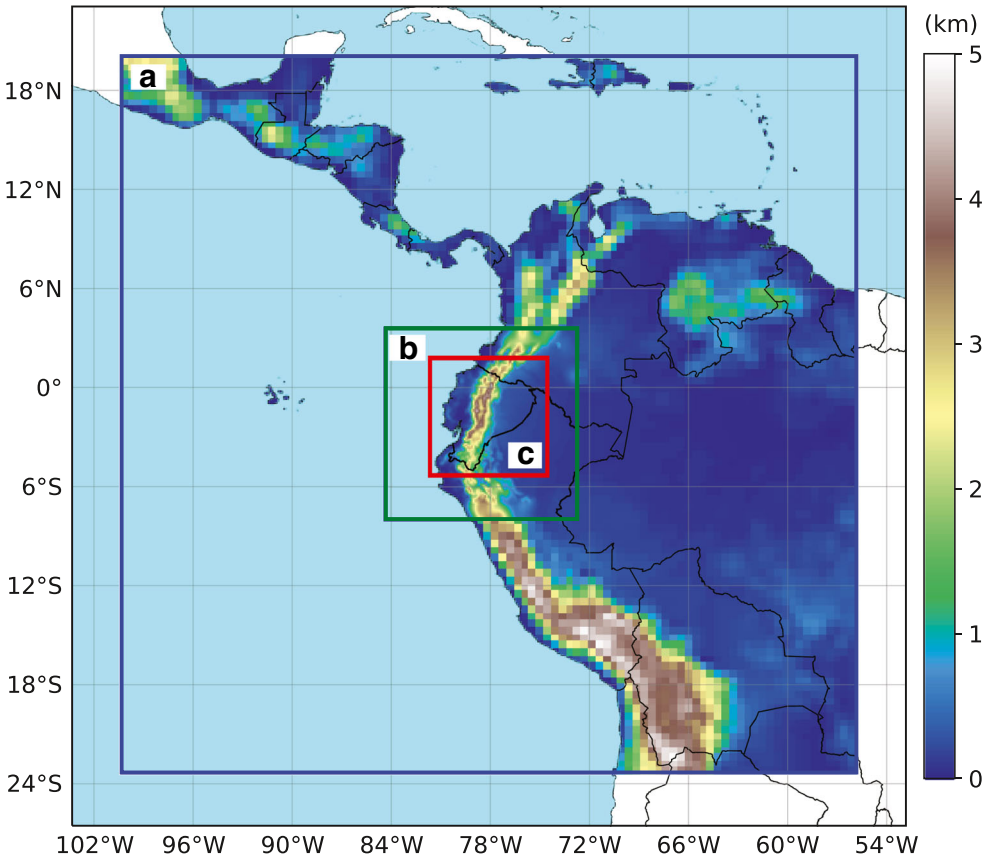

Fig. 1 Domains used in the different experiments. (a) Blue square indicates the parent domain of 50 km horizontal resolution used in the GCM-forced simulations (CCSM4-WRF). It has 100 × 100 grid cells, and it is centered at 1.77° S and 78.10° W. (b) Green square is the nested domain in the GCM-forced simulation, and it is almost identical to the single domain in the Reanalysis-forced experiments (CFSR-WRF) which is also centered at 1.77° S and 78.10° W. The negligible difference between the nested and the single domain in CFSR is due to the downscaling step used in the nested domain which results in small differences in the coordinates values (less than ~ 10^{-5}°, ~ 10^{-3} km). In both experiments, these domains have 130 × 130 grid cells. (c) Red square represents the study domain for CFSR-WRF and CCSM4-WRF experiments, and it is a subset of the nested domain having 80 × 80 grid cells. The topography corresponds to the model topography interpolated to 50 km and 10 km resolution for the parent and nested domain, respectively. Note the transition zone (smoothed) in the nested domain over the Andes close to the northern and southern boundaries

Community Atmosphere Model (CAM) version 5.1 microphysics scheme (Eaton 2011; Neale et al. 2012), and the New Tiedtke cumulus scheme, which is a modified version of the one proposed by Tiedtke (1989) and implemented by Zhang et al. (2011). The longwave and shortwave radiation inputs were set to be solved by new versions of the Rapid Radiative Transfer Model (RRTM; Mlawer et al. 1997) schemes, which have been used in several studies in South America (e.g., Mourre et al. 2016; Junquas et al. 2018; Martinez-Castro et al. 2019; Moya-Alvarez et al. 2019; Campozano et al. 2020). The planetary boundary layer scheme used here is the one developed by Yonsei University (Hong et al. 2006) and has also been widely used in WRF simulations over the Andes of Peru and Ecuador (Mourre et al. 2016; Junquas et al. 2018; Moya-Alvarez et al. 2018, 2019; Martinez-Castro et al. 2019; Campozano et al. 2020). The selected land-surface model is the Unified Noah model (Tewari et al. 2004; Chen and Dudhia 2001), which has been successfully applied in WRF simulations over the tropical Andes (Mourre et al. 2016; Junquas et al. 2018; Moya-Alvarez et al. 2019; Martinez-Castro et al. 2019; Campozano et al. 2020). The atmospheric surface layer scheme used here is based on the Monin-Obukhov similarity theory, which was equally successfully applied to WRF simulations over the tropical Andes in prior studies (Junquas et al. 2018; Campozano et al. 2020). A summary of the main parameterization employed in this study is shown in Table 1.

2.2 The CFSR-WRF simulation

The driving boundary conditions for the reanalysis-based simulation were obtained from the Climate Forecast System Reanalysis (CFSR; Saha et al. 2010a,b), a coupled atmosphere–ocean–land surface–sea ice system with 38 km horizontal resolution and vertical spacing at 64 pressure levels. To our knowledge, this is the first study applying this reanalysis data set over the region of interest, since most prior RCM studies that focused on present-day climate over the tropical Andes relied on the European Centre for Medium-Range Weather Forecasts (ECMWF) reanalysis (ERA-40 or ERA-Interim) (McGlone and Vuille 2012; Martinez et al. 2019). However, several studies have shown that CFSR reproduces the precipitation annual cycle over the Andes reasonably well (Silva et al. 2011; Eichler and Londoño 2013; Blacutt et al. 2015) and it is routinely being applied with good results in WRF-based downscaling studies over North America (e.g., Meyer and Jin 2016) and regions with complex terrain (e.g., Norris et al. 2019). Downscaling CSFR in WRF also appears to outperform other reanalysis products, such as 20CRv2c or ERA20C, when simulating daily precipitation, and it has been shown to faithfully reproduce precipitation in WRF with only a small bias (Toride et al. 2019).

With the parameters selected in Section 2.1, we carried out a 30-year simulation using CFSR as boundary conditions for WRF (CFSR-WRF). The period of simulation ranges from 1979 to 2010. The first year of the simulation was discarded to allow the RCM to spin up the soil temperature (e.g., Bruyère et al. 2015). This simulation was then analyzed in detail by comparing it to in situ observations of temperature and precipitation, in order to validate the model's ability to faithfully reproduce observed changes in climate over Ecuador, both in space and time.

2.3 The CCSM4-WRF simulations

All models produce results with an associated uncertainty that is inherently related to the mathematical formulation of the equations that describe the atmospheric processes implemented in the model and to the numerical methods used to solve these equations. One way to reduce this uncertainty is to consider an ensemble result from multiple models. As Buytaert et al. (2010) suggested, it would be ideal to implement an ensemble of RCMs driven by most of the Coupled Model Intercomparison Project Phase 5 (CMIP5; Taylor et al. 2012) or CMIP6 models. This approach, however, is impractical at this moment in time, because of the high computational demand that a set of such simulations would require. There are more than 40 CMIP5/6 models, several of them with different flavors or members. Also, each member consists of one

Table 1 List of the physical parameterizations used in the WRF simulations

Physical process/variables	Parameterization	Reference
Cloud Microphysics	CAM V5.1	Eaton (2011)
Longwave radiation	RRTM	Mlawer et al. (1997)
Shortwave radiation	RRTM	Mlawer et al. (1997)
Surface layer	MM5 similarity/Monin-Obukhov	Jiménez et al. (2012)
Land surface	Noah land surface model	Chen and Dudhia (2001)
Planetary boundary layer	Yonsei University	Hong et al. (2006)
Cumulus parameterization	New Tiedtke	Zhang et al. (2011)

historical run and 3 or 4 future scenarios. Hence, taking into account only one member per model and 2 future scenarios would require carrying out 120 long simulations (covering at least a couple of decades).

Here we chose a different approach by selecting a GCM which comes with several advantages when performing regional climate studies. This GCM is the member 6 of the Community Climate System Model version 4 (CCSM4; Gent et al. 2011), which is a subset of the Community Earth System Model (CESM). The CCSM4 simulations of global temperature and precipitation patterns are ranked among the top CMIP5 models when compared with observations (Knutti et al. 2013; Bruyère et al. 2015). Furthermore, a post-processed product from this GCM was specifically designed to conduct RCM experiments with WRF (Bruyère et al. 2015). This data set, known as the NCAR CESM Global Bias-Corrected CMIP5 Output to Support WRF/MPAS Research (Monaghan et al. 2014), corresponds to the member 6 of CCSM4, and it has been bias-corrected and post-processed to drive the WRF model (Bruyère et al. 2015). Chimborazo (2018) compared member 6 of CCSM4 for the Ecuadorian region under the RCP8.5 scenario, for the period 2041–2070, with the results from 42 other CMIP5 models, comprising a multi-model ensemble of 98 members. They were able to show that CCSM4 member 6 simulates future changes in temperature and precipitation that are close to the median and mean values of the CMIP5 multi-model ensemble over Ecuador. Hence, we are confident that the results provided by the CCSM model are close to the median of all CMIP5 models over Ecuador and can be considered representative of a broader multi-model ensemble.

Here we conducted three long WRF simulations driven by this data set, referred to as CCSM4-WRF. The first simulation corresponds to the downscaling of historical and present-day climate spanning the late twentieth century from 1975 to 2005. The other two experiments were driven by the RCP4.5 and RCP8.5 scenarios respectively, spanning the period 2040–2070. As in CFSR-WRF, the first year of the simulation was discarded before analysis.

The future climate change signal would be more pronounced and significant, and therefore easier to detect and analyze, if one were to focus on the climate response at the end of the century, once the signal-to-noise ratio of the anthropogenic signal would be much larger. Regional stakeholders and decision-makers involved in climate change adaption, however, do not plan or implement such measures with a 50- to 80-year planning horizon (e.g., Buytaert et al. 2010; Vuille 2013). We therefore decided to focus on the mid-century response (2041–2070), allowing for a 20- to 50-year planning horizon. Campozano et al. (2020) in their analysis of projected future changes in drought conditions over Ecuador came to similar conclusions and also focused on this same time period of analysis.

2.4 Observational data sets

The present-day model simulations of precipitation for both CSFR-WRF and CCSM4-WRF were validated with gridded daily precipitation data from the Climate Hazards Infrared Precipitation with Stations (CHIRPS) data set version 2.0 (Funk et al. 2015). This data set is available at 0.05° × 0.05° starting in 1981. Prior to comparison with the WRF model output, the data was resampled to a 10 × 10-km grid. CHIRPS data have been tested extensively over the Andes region, with very good results (e.g., Rivera et al. 2018; Segura et al. 2019, 2020) and have also been used for WRF model validation over the Andes in previous studies (e.g., Heredia et al. 2018; Martinez, et al. 2019; Martinez-Castro et al. 2019).

For validation of temperature we employ the Climatic Research Unit—University of East Anglia (CRU TS v 4.03) gridded temperature data (Harris et al. 2020). CRU data has been employed to validate temperature in RCM simulations over the tropical Andes by Urrutia and Vuille (2009) and McGlone and Vuille (2012). The main deficiency in the CRU data over the Andes is related not only to the reduced station density (Vuille et al. 2003; McGlone and Vuille 2012) but also to a warm bias at high elevations, when compared with in situ station data, due to the lower elevation of the topography underlying the CRU spatial interpolation scheme (Urrutia and Vuille 2009). CRU TS v 4.03 data is provided at 0.5° resolution and was resampled to a 10 × 10-km resolution prior to comparison with the WRF model output.

Finally, we also compared the simulated precipitation from CFSR-WRF and CCSM4-WRF with selected station data provided by the Ecuadorian National Meteorological and Hydrological Service (Instituto Nacional de Meteorología e Hidrología; INAMHI). While CHIRPS and CRU data are better suited for the model validation in space, given that their data is provided on a spatially complete grid, in situ stations are still useful to assess the ability of WRF to accurately simulate the temporal evolution of precipitation and temperature at specific locations on intraseasonal, seasonal, and interannual timescales. In Chimborazo (2018), data from 42 in situ stations were used for the model validation at individual locations. Here, we only show one example each from a station, representative of low- and high-elevation sites in Ecuador, respectively, to document the consistent temporal evolution between observed and simulated precipitation and temperature.

2.5 Model validation and bias correction

We calculate both Spearman's and Pearson's correlation coefficients and the bias between observations and model output to validate the present-day simulations CFSR-WRF and CCSM4-WRF. The bias was calculated as the average

precipitation or temperature difference between the observation and the model data of the corresponding cell. In the case of the gridded data sets CRU TS v 4.03 and CHIRPS, this calculation was performed on corresponding grid cells, after the observational data sets had been resampled to the WRF resolution. In the case of station data, we chose the model grid cell located closest to the station for comparison with the in situ data. This calculation was performed separately for the four seasons December–February (DJF), March–May (MAM), June–August (JJA), and September–November (SON). However, given the minimal thermal seasonality at the equator, the temperature results are almost identical in each season (not shown) and we therefore restrict the discussion to the annual mean. When analyzing the bias or differences between future and present-day temperature or precipitation fields, a Student *t* test was applied to highlight regions where differences between observed and simulated climate fields (bias) or between present-day and future climate fields (changes in future projections) were statistically significant at the 95% level. These regions are indicated by hatching in the figures.

Since WRF exhibits a significant wet bias in simulated precipitation over the Andes (see section 3.1), we applied a bias correction to the CCSM4-WRF simulation for both the RCP4.5 and RCP8.5 scenarios to obtain more accurate estimates of future precipitation amounts. The wet bias along the Andes is a well-known problem with RCM's when applied over the Andes and several approaches on how to correct for such a bias in RCM's over the Andes have been proposed (e.g., Buytaert et al. 2010; Heredia et al. 2018). Here we apply the Bias Correction (BC) method discussed in Ho et al. (2012), which corrects the projected future (2041–2070) daily precipitation in CCSM4-WRF RCP4.5 and RCP8.5 using the differences in the mean and variability between CCSM4-WRF and CHIRPS observations during the present-day reference period (1976–2005). Hence, we apply the more generalized version of this method, which carries the advantage of not only correcting the mean values, but also the temporal variability of the simulated precipitation, in accordance with the behavior of the observed CHIRPS precipitation (Ho et al. 2012). According to this BC method, the future bias-corrected precipitation $P_{\mathrm{BC(RCP4.5;8.5)}}$ is calculated as follows:

$$P_{\mathrm{BC(RCP4.5;8.5)}} = P_{\mathrm{OBS}} + \frac{\sigma_{\mathrm{OBS}}}{\sigma_{\mathrm{WRF(CTRL)}}}\left(P_{\mathrm{WRF(RCP4.5;8.5)}} - P_{\mathrm{WRF(CTRL)}}\right) \quad (1)$$

where P_{OBS} is the observed CHIRPS precipitation during the reference period (1981–2005), and $\sigma_{\mathrm{WRF(CTRL)}}$ and σ_{OBS} represent the standard deviation of the WRF-CCSM4 and CHIRPS precipitation data during the reference period, respectively. $P_{\mathrm{WRF(CTRL)}}$ represents the WRF-CCSM4 precipitation from the reference period, while $P_{\mathrm{WRF(RCP4.5;8.5)}}$ represents the simulated WRF-CCSM4 precipitation for the future period under either the RCP4.5 or RCP8.5 scenario.

We did not perform a bias-correction for the simulated temperature fields, because we are mostly interested in the relative future temperature changes and how they depend on elevation (i.e., EDW analysis). For such an analysis, the absolute future temperature is irrelevant. Furthermore, the apparent bias documented in the temperature fields simulated by CCSM4-WRF is largely an artifact of the higher-resolution topography underlying the simulation (see section 3.1). In addition, the CRU TS v 4.03 data used for validation suffers from its own warm bias at high elevations and any attempt to bias-correct the temperature fields would therefore likely introduce additional uncertainty.

3 Results

3.1 Simulating present-day climate with CFSR-WRF and CCSM4-WRF

Figure 2 shows a comparison between mean annual temperature in observations from CRU TS v 4.03 with CFSR-WRF and CCSM4-WRF, respectively. Note that the two observational fields from CRU TS v 4.03 (Fig. 2a, d) are slightly different due to the different time period of analysis (1981–2010 for CFSR-WRF and 1976–2005 for CCSM4-WRF). Both simulations show similar patterns, with a negative temperature bias at low elevations and in the high Andes and a positive bias along the lower elevations of the eastern and western Andean slopes (Fig. 2c, f). Interestingly, the cold bias in the lowlands is more pronounced in CFSR-WRF, while it is small in CCSM4-WRF. While this cold bias at low elevations is likely real, much of the temperature bias along the Andean slopes and at high elevations can be attributed to the differences in resolution between the two products. After all, the surface temperature depends on the underlying topography, which is different between CRU TS v 4.03 and our WRF simulations. Indeed, if one calculates the lapse rate based on the underlying topography, it is quite similar between the different products but suggests that CRU TS v 4.03 (− 0.0048 K m^{-1}) has a slightly reduced temperature lapse rate compared with CFSR-WRF (− 0.0052 K m^{-1}) and CCSM4-WRF (− 0.0055 K m^{-1}). This is consistent with results by Urrutia and Vuille (2009) who documented that CRU exhibits a warm bias over the Andes, when compared with in situ station data. Hence, the apparent cold bias in the high Andes displayed by WRF, is a combination of two factors: the higher elevation of the Andes in the WRF simulations as compared with CRU TS v 4.03 and a warm bias of CRU TS v 4.03 at high

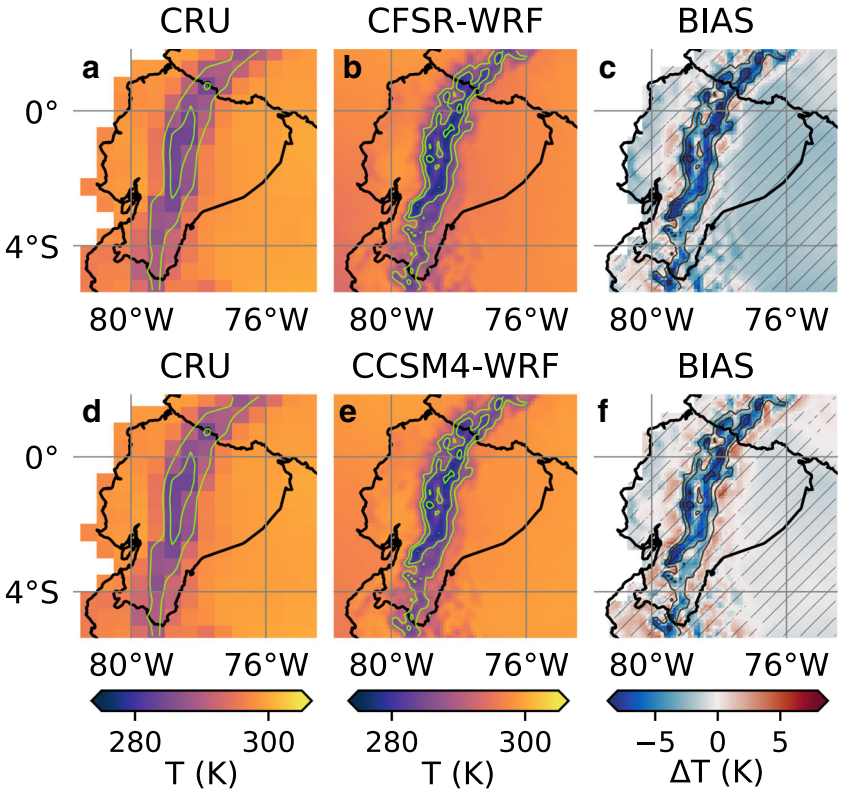

Fig. 2 **a** Observed annual mean surface air temperature (in K) based on CRU TS v 4.03 (1981–2010). **b** as in **a** but for CFSR-WRF. **c** Difference between CRU TS4 v 4.03 and CFSR-WRF (Bias). **d** as in **a** except for period 1976–2005. **e** as in **b** but for CCSM4-WRF (1976–2005). **f** Difference between CRU TS4 v 4.03 and CCSM4-WRF (Bias). Hatching in **c** and **f** indicates regions where bias is significant at $p < 0.05$. Contour lines are shown every 1000 m, starting at 2000 m a.s.l. Note that CRU TS v 4.03 was resampled to match resolution of WRF prior to calculation of the bias but is shown here in its native 0.5° resolution to highlight its reduced vertical and horizontal resolution when compared with WRF

elevations. This notion is further supported by the fact that the CFSR-WRF lapse rate (− 0.0052 K m^{-1}) is identical to the observed lapse rate in the tropical Andes, determined by Urrutia and Vuille (2009) from station data (− 0.0052 K m^{-1}). Similarly, the warm bias along the Andean slopes also results from the difference in resolution, and hence the shape of the Andean topography between the two products. The CRU TS v 4.03 topography is much smoother, with an Andean mountain range that is considerably wider (Fig. 2a, d), while WRF more accurately resolves the true topographic characteristics of the steep and narrow Andean mountain range (see differences in topography displayed by contours in Fig. 2). As a result, the elevation of CRU grid cells along the lower elevations on each side of the Andes is too high, resulting in an apparent warm bias of the WRF simulations.

Aside from the spatial representation of temperature in WRF, we also considered the ability of the model to reproduce its observed temporal variability. For this analysis, we chose select stations from the INAMHI meteorological network that are representative of coastal and Andean settings, respectively. Pearson's and Spearman's correlation coefficients were calculated to assess the skill of the model in reproducing the observed temperature variability.

Figure 3 a and b show a comparison between simulated and observed temperature at daily (Fig. 3a) and monthly resolution (Fig. 3b) for station M0005 (Portoviejo-UTM, 1.04° S, 80.46° W, 59 m a.s.l.), located in the coastal region. The temporal structure of air temperature variability over the historical period is adequately captured at both daily, monthly, and interannual time scales. For instance, the similarity in the temporal evolution of the warming associated with El Niño events (1982/1983, 1997/1998, and 2010) is evident at both daily and monthly resolutions. We do not expect that the daily correlation coefficient be high, due to the limited temporal predictability of daily weather conditions in the model. However, at monthly resolution, the influence of the lateral boundary conditions, in particular Pacific sea surface temperature (SST), becomes more notable, resulting in increased correlation coefficients. Figure 3 c and d present a similar analysis for station M0004 (Rumipamba-Salcedo, 1.02° S, 78.59° W, 2685 m a.s.l.), located in the Andes, demonstrating the good performance of CFSR-WRF in reproducing the observed temperature variability in the Andes of Ecuador.

Figures 4 and 5 show the comparison of CFSR-WRF and CCSM4-WRF with CHIRPS precipitation data, respectively, for each season. Note that the time period of analysis is again slightly different for the 2 simulations (1981–2010 for CFSR-WRF and 1981–2005 for CCSM4-WRF). Therefore, the CHIRPS results, while very similar, are not identical between Figs. 4 and 5. The general march of the seasonal cycle with enhanced precipitation in DJF and drier conditions in JJA and SON along the Pacific coast, and a main wet season in MAM and JJA over the Ecuadorian Amazon region is correctly reproduced by both WRF simulations. In general, however, the WRF simulations tend to produce a dry bias in the

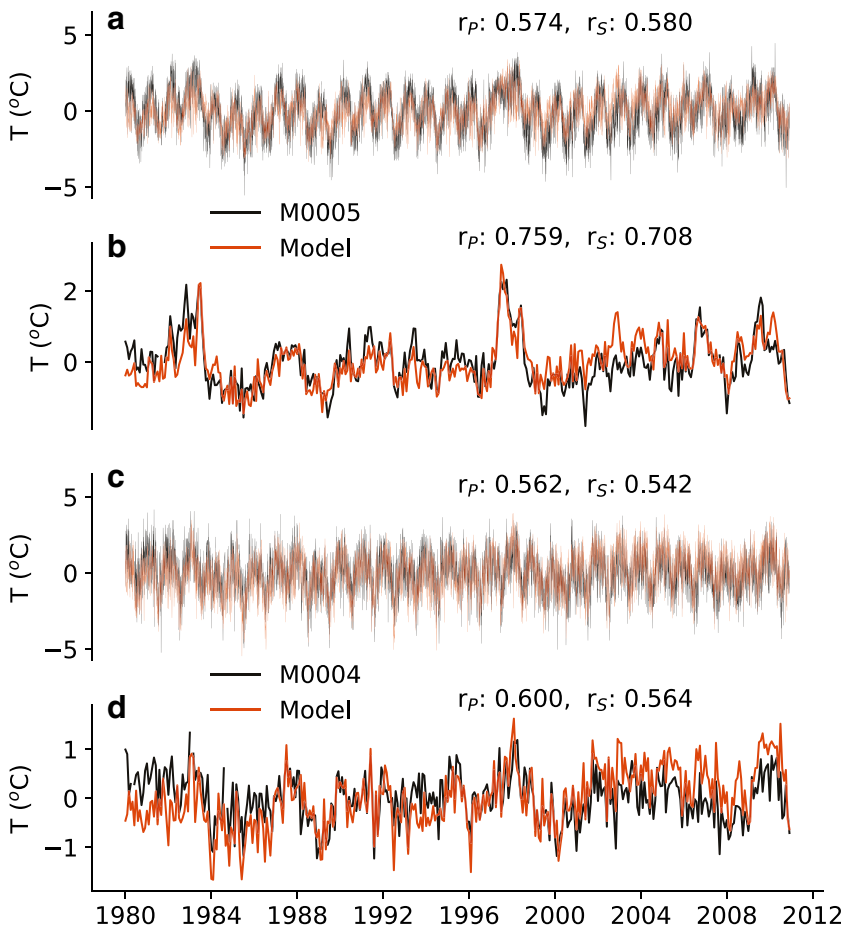

Fig. 3 Comparison between simulated (CFSR-WRF) and observed (station data) air temperature. Black line indicates observations at station M0005 (Portoviejo-UTM, coastal region, 59 m a.s.l.), and orange line shows model data from grid cell encompassing station M0005. **a** daily resolution and **b** monthly anomalies. Note that long-term mean has been removed from both data sets. r_P and r_S are the Pearson's and Spearman's correlation coefficients, respectively. **c** and **d** as in **a** and **b** but for station M0004 (Rumipamba-Salcedo, Mountain region, 2685 m a.s.l.)

lowlands, especially in DJF and MAM but also in JJA on the Amazon side. In the Andes, on the other hand, and especially on the eastern slopes, the WRF simulations overestimate precipitation amounts. In general, both the dry and the wet bias tend to be more pronounced in CCSM4-WRF.

Figure 6 shows the comparison between precipitation in the CSFR-WRF model and observations for the same stations as in Fig. 3, documenting that the model, when driven with reanalysis boundary conditions, is able to quite faithfully reproduce the seasonality and interannual variability of precipitation. While the correlation at the daily time step is quite low, the intraseasonal and interannual variability is accurately simulated by the model as highlighted by the wet anomalies during the 1982–1983 and 1997–1998 El Niño events at the lowland station M0005.

3.2 Projected temperature change under RCP4.5 and RCP8.5

Figure 7 shows the projected change in annual mean temperature for the RCP4.5 and 8.5 scenarios, respectively. The projected changes are calculated as the difference between the annual mean temperature of the periods 2041–2070 and 1976–2005. In the RCP4.5 scenario a general warming over the entire continental part of the domain is apparent, with larger warming over the Guayas River basin (80–79° W, 1–2° S) and along the Andes, reaching a maximum warming of 1.6 K. It is notable that the coastal ocean, which also influences the coastal land areas, is projected to cool by up to − 0.8 K. This cooling most likely reflects internal multi-decadal variability in the particular CCSM4 simulation used to drive the WRF model, which by the middle of the twenty-first century is still able to dominate over the rather muted greenhouse gas forcing in RCP4.5 (Deser et al. 2012; Thompson et al. 2015). Indeed, Pacific decadal variability has a very strong influence on climate along the west coast of South America with the recent cold phase of the Pacific Decadal Oscillation (PDO) leading to a significant cooling trend in coastal areas of the west coast of South America during the past three decades (Vuille et al. 2015) and also significantly affecting precipitation over Ecuador (Mora and Willems 2012). This aspect reinforces the notion that ideally future projections should be based on large ensembles of climate change simulations to cancel out internal variability, but as discussed above, in the case of dynamical downscaling this is largely impractical. It is also noteworthy, however, that a future cooling in the eastern

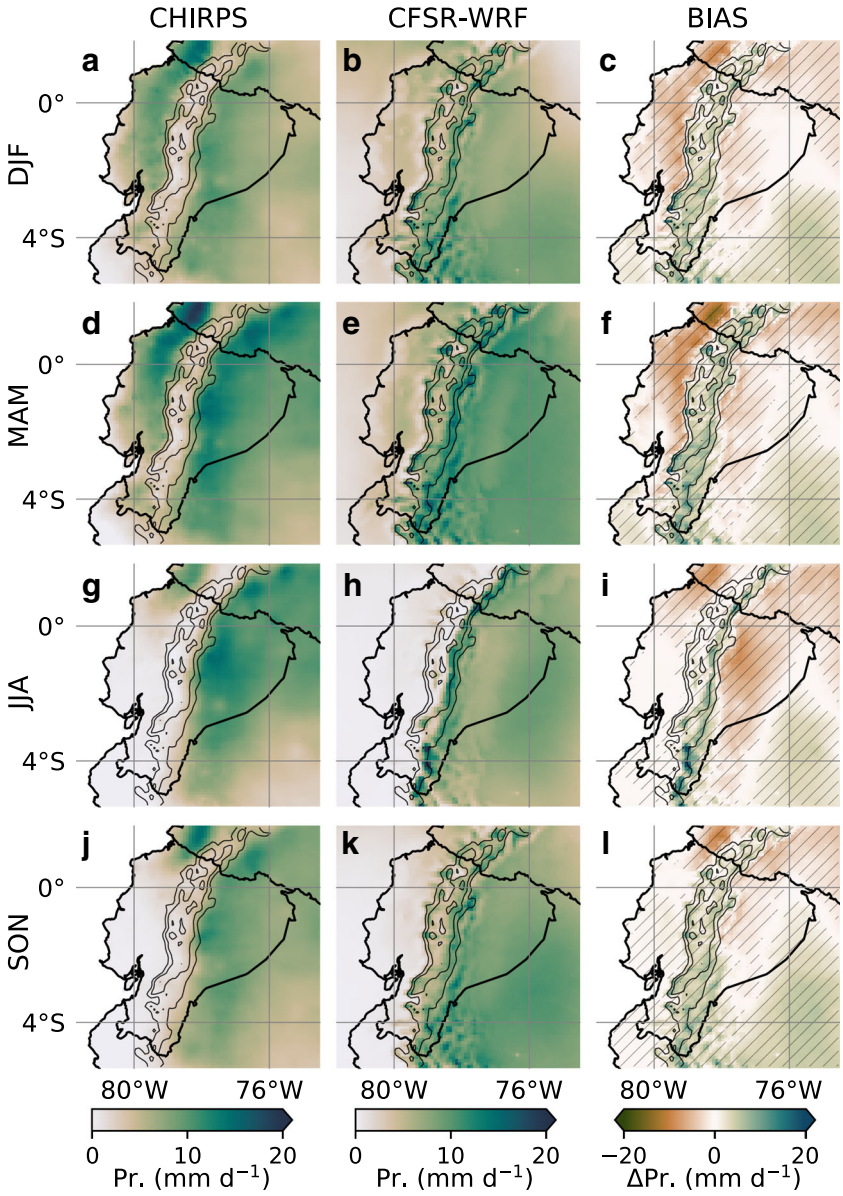

Fig. 4 **a** Observed DJF precipitation (in mm day^{-1}) based on CHIRPS (1981–2010). **b** as in **a** but for CFSR-WRF. **c** Difference between CHIRPS and CFSR-WRF (Bias). **d–f** as in **a–c** except for MAM. **g–i** as in **a–c** except for JJA. **j–l** as in **a–c** except for SON. Hatching in **c**, **f**, **i**, and **l** indicates regions where bias is significant at $p < 0.05$. Contour lines are shown every 1000 m, starting at 2000 m a.s.l

Pacific is not necessarily inconsistent with a forced response to increased greenhouse gas concentrations, as the increased radiative forcing may result in a strengthened Southeast Pacific anticyclone, stronger alongshore coastal winds, and hence enhanced upwelling of cold water off the coast of South America (e.g., Falvey and Garreaud 2009; Goubanova et al. 2011). In either case, the influence of the cool SST off the coast of Ecuador in the RCP4.5 scenario leads to reduced warming along the coast, but does not seem to affect the warming rate further inland. On the other hand, the temperature projection based on the RCP8.5 scenario shows significant warming over the whole domain. Most of the coastal region is subject to a warming of ~ 1.6 K, while in the Andes, temperature would increase by more than 2.0 K, with an apparent enhanced warming at higher elevations.

To further analyze how future warming depends on elevation and whether the warming rates are comparable on both sides of the Andes, we plot the projected future temperature change at each grid cell as a function of the grid cell's elevation in Fig. 8. We exclude data points below 500 m as they are too far removed from the Andes and lead to large scatter at very low elevations. We further distinguish between temperature trends on the eastern and western Andean slopes, since (a) they are influenced by different large-scale forcings, (b) early observational studies detected different temperature trends between the two slopes of the Andes (Vuille and Bradley 2000; Vuille et al. 2003), and (c) it has been suggested that the two sides might also see different future elevation-dependent warming trends (Urrutia and Vuille 2009). As shown in Fig. 8, temperature will increase by mid-century in

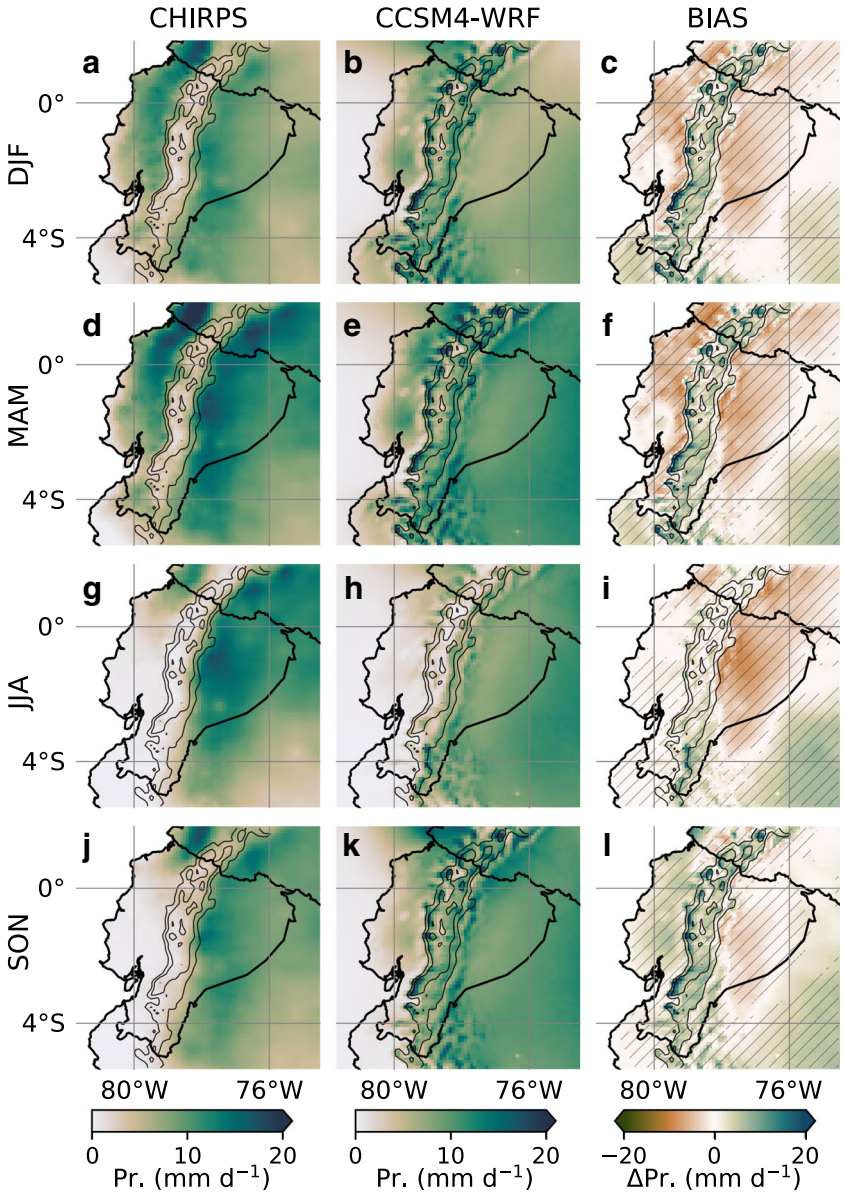

Fig. 5 **a** Observed DJF precipitation (in mm day^{-1}) based on CHIRPS (1981–2005). **b** as in **a** but for CCSM4-WRF. **c** Difference between CHIRPS and CCSM4-WRF (Bias). **d–f** as in **a–c** except for MAM. **g–i** as in **a–c** except for JJA. **j–l** as in **a–c** except for SON. Hatching in **c**, **f**, **i**, and **l** indicates regions where bias is significant at $p < 0.05$. Contour lines are shown every 1000 m, starting at 2000 m a.s.l

both scenarios and there is a clear elevation-dependence of the warming, with larger warming at higher elevation. In both scenarios and on both sides of the Andes, the elevation dependence (i.e., the slope of the EDW regression line) is significantly different from zero ($p < 0.01$), indicating that the degree of future warming does indeed depend on elevation. Interestingly, the EDW is also significantly different between the two slopes ($p < 0.01$) in both scenarios. The increase of the warming with elevation is more pronounced on the western side (RCP4.5: 0.11 K km^{-1}; RCP8.5: 0.16 K km^{-1}), while it appears more muted to the east (RCP4.5: 0.07 K km^{-1}; RCP8.5: 0.09 K km^{-1}). The elevation-dependent warming simulated for the western side of the Andes is consistent with findings by Urrutia and Vuille (2009) who found a similar EDW effect in their analysis of a RCM run under a high-emission scenario. However, in their study, the EDW effect on the eastern side was restricted to elevations above 2000 m, as the lowest elevations over western Amazon basin saw even stronger warming. The results, however, are difficult to compare quantitatively between the two studies, as the simulations performed by Urrutia and Vuille (2009) encompassed a much larger spatial domain, focused on the end of the twenty-first century, were based on a different model with much coarser resolution (50 km) and were forced with an older Special Report on Emissions Scenario (SRES-A2) emission pathway.

3.3 Projected precipitation change under RCP4.5 and RCP8.5

Figure 9 shows the projected future precipitation changes under both emission scenarios. In the case of RCP4.5, precipitation is projected to decrease over the coastal region, while

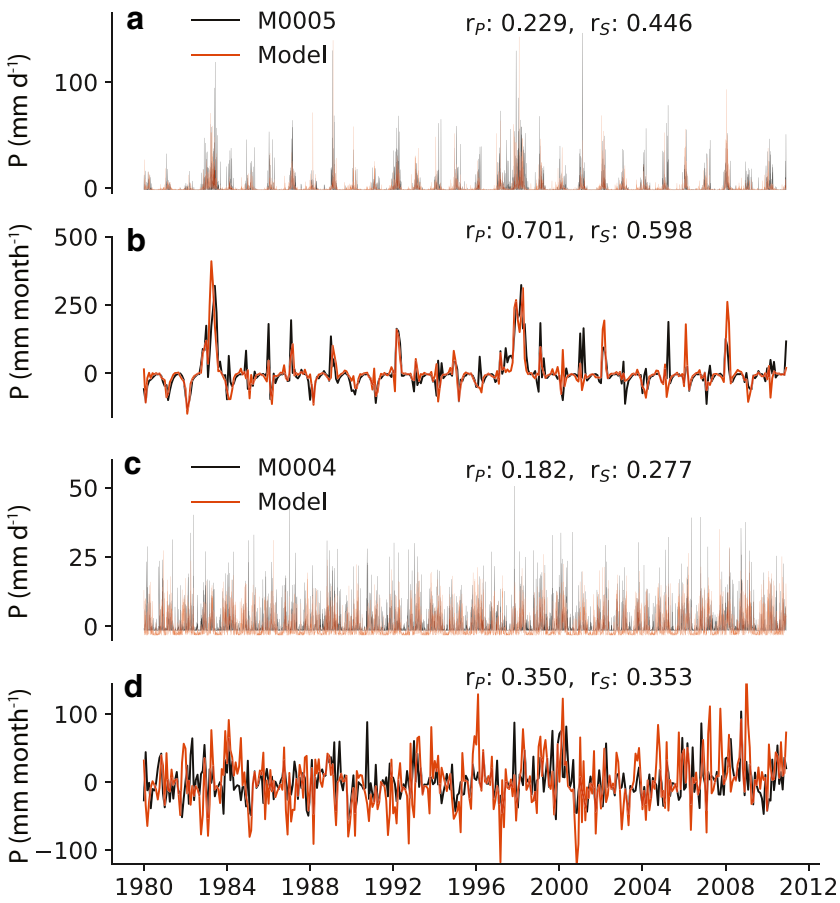

Fig. 6 Comparison between simulated (CFSR-WRF) and observed precipitation from station data. Black line indicates observations at station M0005 (Portoviejo-UTM, coastal region, 59 m a.s.l.), and orange line shows model data from grid cell encompassing station M0005 at **a** daily resolution and **b** for monthly anomalies. r_P and r_S are the Pearson's and Spearman's correlation coefficients, respectively. **c** and **d** as in **a** and **b** but for station M0004 (Rumipamba-Salcedo, Andes region, 2685 m a.s.l.)

slightly wetter conditions are expected over the Andes, especially along the eastern range of the Andes during the JJA season. The Amazon region is also projected to become slightly wetter in DJF and MAM, but slightly drier in the other two seasons. The coastal drying in RCP4.5 is consistent with the cooling off the coast discussed above, as the increased stability of the coastal atmosphere will trap moisture below a low-level inversion, which will aid in significantly reducing convective activity and moisture influx toward the inland areas (García-Garizábal 2017). The RCP8.5 scenario shows a more complex situation for the different seasons. The coastal region is projected to become wetter than present in DJF and MAM, while the western Andean foothills will experience little change in DJF, but drying in MAM. No major changes in precipitation are projected for JJA and SON over the coastal region. Over the Andes, conditions are projected to become more humid in DJF, MAM, and JJA, especially along the eastern range of the Andes. SON is the only season, which presents slightly drier future conditions in the Andes of Ecuador. The Amazon region is generally not projected to

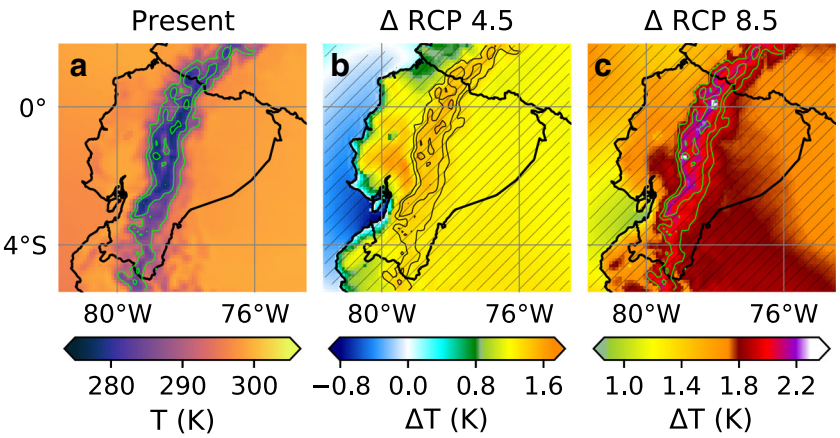

Fig. 7 Annual mean projected temperature change for the period 2041–2070 for the CCSM4-WRF simulations compared with the present-day climate (**a** 1976–2005) for **b** RCP4.5 and **c** RCP8.5 scenarios. Note that the plots have different scales and an adjusted color map for both scenarios in order to improve readability. Hatching in **b** and **c** indicates regions where projected temperature change is significant at $p < 0.05$. Contour lines are shown every 1000 m, starting at 2000 m a.s.l

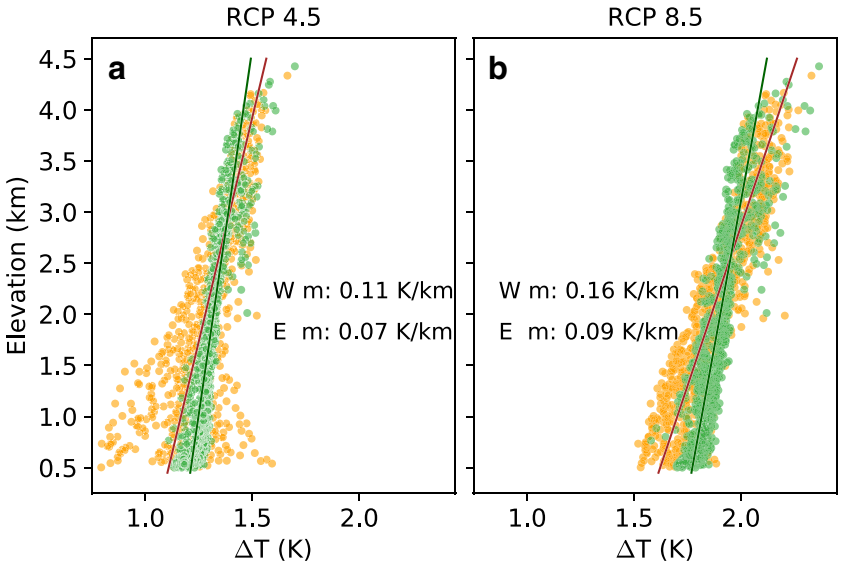

Fig. 8 Projected future temperature change (2041–2070 minus 1976–2005) vs. altitude for western (orange dots) and eastern (green dots) slopes of the Andes for **a** RCP4.5 and **b** RCP8.5. The solid lines represent the linear regression with slopes (m) shown by the W m and E m values for the western and eastern sides respectively. Temperature trends are significant at $p < 0.05$ at all elevations

undergo major changes in precipitation amounts, although there is a slight drying projected for JJA and SON, while the eastern Andean foothills display wetter future conditions according to our simulations.

Given the significant precipitation bias produced by CCSM4-WRF, especially along the Andean slopes, we also present maps of bias-corrected future annual mean precipitation totals. Figure 10 compares the observed present-day precipitation from CHIRPS with both the raw and bias-corrected CCSM4-WRF precipitation fields for the middle of the twenty-first century under both emissions pathways. The results suggest that the most significant future impact on precipitation in Ecuador under the low-emission scenario RCP4.5 is restricted to northwestern Ecuador, where our simulation suggests enhanced future drying (compare Fig. 10 a and c). However, given that this result stems from the oceanic cooling simulated by CCSM4-WRF, it should be interpreted with caution. Precipitation amounts over the Andes and the Amazon basin are not projected to change drastically. Under the RCP8.5 scenario, the impacts on total annual precipitation are rather minimal to the east of the Andes or in the Andes themselves, while the lower elevations on the eastern Andean slopes are projected to see an increase in future precipitation, even after the model-induced wet bias over this region is removed (compare Fig. 10 d and f).

4 Discussion and conclusions

The main objective of this study was to contribute to the ongoing development of a modeling framework for studying present and future climate change over Ecuador. Four 30-year simulations were carried out with a high spatial (10 km, 51 vertical levels) and temporal (6h) resolution, allowing

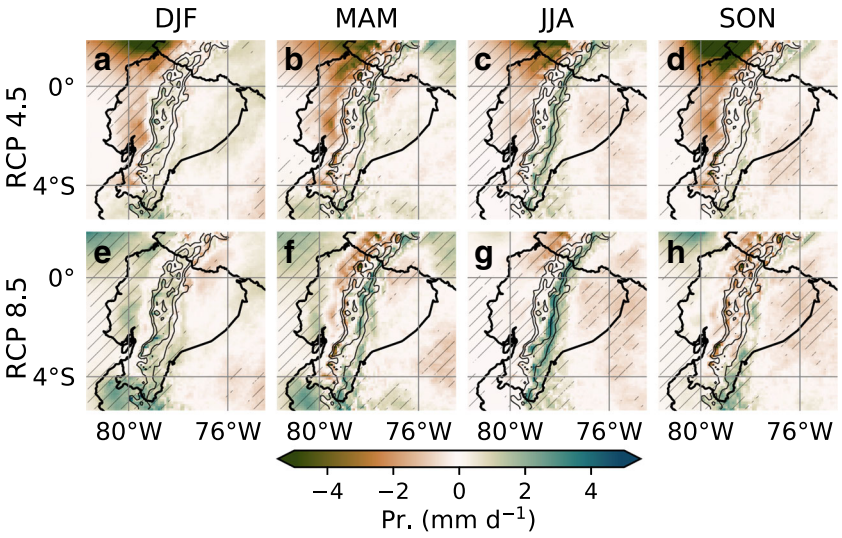

Fig. 9 Projected seasonal precipitation changes for the period 2041–2070 in the CCSM4-WRF simulations compared with the present-climate (1976–2005) for RCP4.5 (top row) and RCP8.5 (bottom row) scenarios. Hatching indicates regions where projected precipitation changes are significant at $p < 0.05$. Contour lines are shown every 1000 m, starting at 2000 m a.s.l

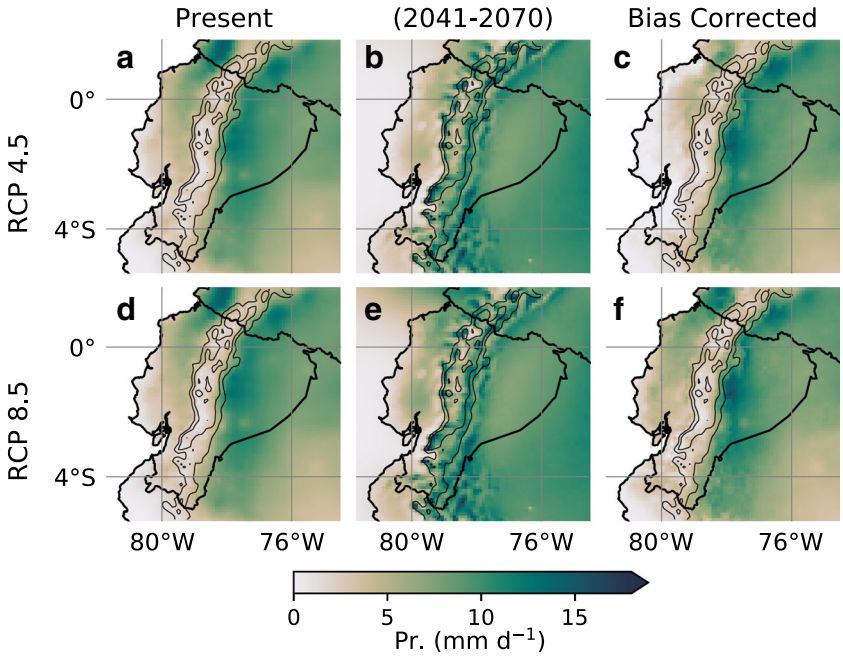

Fig. 10 Comparison of observed annual mean precipitation for present-day (CHIRPS 1981–2005—left column), projected annual mean precipitation for the period 2041–2070 in the CCSM4-WRF simulations (middle column) and bias-corrected projected annual mean precipitation for the period 2041–2070 in the CCSM4-WRF simulations (right column) for RCP4.5 (top row) and RCP8.5 scenarios (bottom row). Contour lines are shown every 1000 m, starting at 2000 m a.s.l

detailed hydrometeorological analyses over the Andes in both space and time domains.

Our simulations with CFSR-WRF document that the model exhibits reasonable skill in realistically simulating climate variability from daily to interannual time scales over continental Ecuador. The comparison between temperature anomalies from CRU TS v 4.03 and CFSR-WRF shows a large apparent cold bias over the Andes, but much of this bias can be attributed to the differences in the underlying topography between the two products; a result that was also documented in prior studies (e.g., Urrutia and Vuille 2009). The temporal evolution of temperature is well simulated by CFSR-WRF on multiple time scales, as documented by the comparison with in situ observations from both the coastal and Andean region.

The seasonal cycle of precipitation is also reasonably well simulated over the coastal, Andean and Amazon regions of Ecuador in both CFSR-WRF and CCSM4-WRF. The WRF model does, however, underestimate precipitation in the lowlands and shows a significant wet bias along the eastern Andean slopes, especially when forced by CCSM4. This wet bias over regions with steep orographic gradients is well documented in RCMs employed in the Andes and could potentially be reduced in future studies by applying higher-resolution simulations (Mourre et al. 2016; Moya-Alvarez et al. 2019; Saavedra et al. 2020). The temporal variability of precipitation over Ecuador is reasonably well simulated by the WRF model, both in the Andes and along the coast, especially on interannual time scales, as the model adequately simulates precipitation anomalies induced by ENSO.

Projections of future temperature and precipitation changes document the importance of reducing greenhouse gas emissions over the coming decades, as the warming over the region is significantly reduced under the low emission scenario RCP4.5, when compared with the high emissions scenario RCP8.5. Our study also shows that the warming by the middle of the twenty-first century can surpass an additional 1.5 or even 2.0 K when compared with the end of the twentieth century, especially at the highest elevations, where the warming is most pronounced. This EDW effect is consistent with earlier modeling studies in the tropical Andes (e.g., Vuille et al. 2003; Bradley et al. 2006; Urrutia and Vuille 2009), although the results are difficult to compare between studies, given the differences in domain size, modeling approach, emissions scenarios, and time horizons considered. Nonetheless, the study highlights the ability of WRF to simulate EDW in the tropical Andes, as documented previously for other mountain ranges, such as the Rocky Mountains (Letcher and Minder 2017; Minder et al. 2018). While diagnosing the specific feedbacks that lead to EDW in this part of the world is beyond the scope of this study, it points to the need of better monitoring the highest elevations in the Andes, given the importance of the environmental services provided by high-altitude wetland ecosystems and glaciers (Buytaert et al. 2011; Viviroli et al. 2011; Huss et al. 2017; Vuille et al., 2018).

Bias-corrected future changes in precipitation appear to be rather modest in both RCP4.5 and RCP8.5, but indicate generally drier conditions along the coast in RCP4.5 and slightly wetter conditions along the eastern Andean slopes in both scenarios. Precipitation changes in the interandean valleys are projected to be rather minimal. However, these WRF projections of future precipitation changes need to be interpreted

with caution, even though they are bias-corrected. Multiple studies have documented that the simulated precipitation in the Andes depends on the driving model, the WRF model resolution and the implemented convective parameterization (Mourre et al. 2016; Junquas et al. 2018; Moya-Alvarez et al. 2018; Campozano et al. 2020).

The skill that any model has in reproducing present climate is critical to evaluate its ability to provide reliable future projections. However, there are of course uncertainties associated with the WRF simulations, which stem from a combination of factors, including errors inherited from its driving GCM, errors imposed by WRF and its set of parameterizations, but also uncertainties that are related to the choice of the future emissions scenarios. Notwithstanding these limitations, WRF in particular has proven to be a useful tool for understanding future changes over regions of complex terrain (e.g., Minder et al. 2018) and outperformed other RCMs in intercomparison studies over South America, adding value when compared with the driving GCM (Solman and Blazquez 2019). While the choice of the driving GCM will of course influence the outcome (e.g., Campozano et al. 2020), we selected a GCM that simulates future temperature and precipitation changes over Ecuador that are close to the median of the CMIP5 multi-model ensemble, ensuring that out future projections are unlikely to be outlier results.

Acknowledgments We acknowledge the Instituto Nacional de Meteorología e Hidrología del Ecuador (INAMHI) for providing the historical data from their weather station network. We would like to acknowledge high-performance computing support provided by NCAR's Computational and Information Systems Laboratory, sponsored by the National Science Foundation. CFSR-WRF and CCSM4-WRF were run using their Yellowstone high performance computing system (ark:/85065/d7wd3xhc). We also would like to acknowledge the data access and computing support provided by the NCAR CMIP Analysis Platform (doi:10.5065/D60R9MSP).

Authors' contributions OC ran the WRF simulations. MV and OC designed the study, analyzed, and interpreted the data and wrote the paper.

Funding This research was sponsored by the U.S. State Department (award S-LMAQM-11-GR-0860) and the U.S. National Science Foundation (award OISE-1743738).

Data availability WRF data used in this study will be made available in a public domain site upon acceptance of the manuscript. All other data sets used in this study are publicly available.

Compliance with ethical standards

Competing interests The authors declare that they have no competing interests.

Code availability Python code developed for this study is available from the authors upon request.

References

Blacutt L, Herdies ADL, de Gonçalves LGG, Vila DA, Andrade M (2015) Precipitation comparison for the CFSR, MERRA, TRMM3B42 and combined scheme datasets in Bolivia. Atmos Res 163:117–131. https://doi.org/10.1016/j.atmosres.2015.02.002

Bradley RS, Vuille M, Diaz HF, Vergara W (2006) Threats to water supplies in the Tropical Andes. Science 312(5781):1755–1756. https://doi.org/10.1126/science.1128087

Bruyère CL, Monaghan AJ, Steinhoff DF, Yates D (2015) Bias-corrected CMIP5 CESM data in WRF/MPAS Intermediate File Format. NCAR Technical Note NCAR/TN-515+STR, National Center for Atmospheric Research:60 pp. https://doi.org/10.5065/D6445JJ7

Buytaert W, Célleri R, Timbe L (2009) Predicting climate change impacts on water resources in the Tropical Andes: effects of GCM uncertainty. Geophys Res Lett 36:L07406. https://doi.org/10.1029/2008GL037048

Buytaert W, Vuille M, Dewulf A, Urrutia R, Karmalkar A, Célleri R (2010) Uncertainties in climate change projections and regional downscaling in the tropical Andes: implications for water resources management. Hydrol Earth Syst Sci 14(7):1247–1258. https://doi.org/10.5194/hess-14-1247-2010

Buytaert W, Cuesta-Camacho F, Tobón C (2011) Potential impacts of climate change on the environmental services of humid tropical alpine regions. Glob Ecol Biogeogr 20:19–33. https://doi.org/10.1111/j.1466-8238.2010.00585.x

Campozano L, Vázquez-Patiño A, Tenelanda D, Feyen J, Samaniego E, Sánchez E (2017) Evaluating extreme climate indices from CMIP3&5 global climate models and reanalysis data sets: a case study for present climate in the Andes of Ecuador. Int J Climatol 37:363–379. https://doi.org/10.1002/joc.5008

Campozano L, Ballari D, Montenegro M, Aviles A (2020) Future meteorological droughts in Ecuador: decreasing trends and associated spatio-temporal features derived from CMIP5 models. Front Earth Sci 8:17. https://doi.org/10.3389/feart.2020.00017

Chimborazo O (2018) Projected changes in climate, elevation-dependent warming, and extreme events over continental Ecuador for the period 2041-2070. State University of New York at Albany, (Order No. 13419110). Available from dissertations & theses @ SUNY Albany; ProQuest Dissertations & Theses Global. (2158349782). https://search-proquest-com.libproxy.albany.edu/docview/2158349782?accountid=14166.

Chen F, Dudhia J (2001) Coupling an advanced land surface-hydrology model with the Penn State-NCAR MM5 modeling system. Part I: model implementation and sensitivity. Mon Weather Rev 129:569–585. https://doi.org/10.1175/1520-0493(2001)129<0569:CAALSH>2.0.CO;2

Deser C, Phillips A, Bourdette H, Teng H (2012) Uncertainty in climate change projections: the role of internal variability. Clim Dyn 38(3-4):527–546. https://doi.org/10.1007/s00382-010-0977-x

Eaton B (2011) User's guide to the Community Atmosphere Model CAM-5.1. NCAR. http://www.cesm.ucar.edu/models/cesm1.0/cam/docs/ug5_1/ug.html.

Eichler TP, Londoño AC (2013) South American climatology and impacts of El Niño in NCEP's CFSR data. Adv Meteorol 2013:492630–492615. https://doi.org/10.1155/2013/492630

Falvey M, Garreaud R (2009) Regional cooling in a warming world: recent temperature trends in the southeast Pacific and along the west coast of subtropical South America (1979-2006). J Geophys Res 114:D04102. https://doi.org/10.1029/2008JD010519

Francou B, Vuille M, Favier V, Cáceres B (2004) New evidence for an ENSO impact on low latitude glaciers: Antizana 15, Andes of Ecuador, 0°28'S. J Geophys Res 109:D18106. https://doi.org/10.1029/2003JD004484

Funk C, Peterson P, Landsfeld M, Pedreros D, Verdin J, Shukla S, Husak G, Rowland J, Harrison L, Hoell A, Michaelsen J (2015) The climate hazards infrared precipitation with stations - a new environmental record for monitoring extremes. Sci Data 2:150066. https://doi.org/10.1038/sdata.2015.66

García-Garizábal I (2017) Rainfall variability and trend analysis in coastal arid Ecuador. Int J Climatol 37:4620–4630. https://doi.org/10.1002/joc.5110

Gent PR, Danabasoglu G, Donner LJ, Holland MM, Hunke EC, Jayne SR, Lawrence DM, Neale RB, Rasch PJ, Vertenstein M, Worley PH, Yang ZL, Zhang M (2011) The Community Climate System Model version 4. J Clim 24:4973–4991. https://doi.org/10.1175/2011JCLI4083.1

Goubanova K, Echevin V, Dewitte B, Codron F, Takahashi K, Terray P, Vrac M (2011) Statistical downscaling of sea-surface wind over the Peru-Chile upwelling region: diagnosing the impact of climate change from the IPSL-CM4 model. Clim Dyn 36(7-8):1365–1378. https://doi.org/10.1007/s-0382-010-0824-0

Harris I, Osborn TJ, Jones PD, Lister DH (2020) Version 4 of the CRU TS monthly high-resolution gridded multivariate climate dataset. Sci Data 7:109. https://doi.org/10.1038/s41597-020-0453-3

Hastenrath S, Lamb PJ (2004) Climate dynamics of atmosphere and ocean in the equatorial zone: a synthesis. Int J Climatol 24:1601–1612. https://doi.org/10.1002/joc.1086

Heredia MB, Junquas C, Prieur C, Condom T (2018) New statistical methods for precipitation bias correction applied to WRF model simulations in the Antisana region, Ecuador. J Hydrometeorol 19(12):2021–2040. https://doi.org/10.1175/JHM-D-18-0032.1

Ho CK, Stephenson DB, Collins M, Ferro CA, Brown SJ (2012) Calibration strategies: a source of additional uncertainty in climate change projections. Bull Amer Meteor Soc 93:21–26. https://doi.org/10.1175/2011BAMS3110.1

Hong S, Noh Y, Dudhia J (2006) A new vertical diffusion package with an explicit treatment of entrainment processes. Mon Weather Rev 134:2318–2341. https://doi.org/10.1175/MWR3199.1

Huss M, Bookhagen B, Huggel C, Jacobsen D, Bradley RS, Clague JJ, Vuille M, Buytaert W, Cayan DR, Greenwood G, Mark BG, Milner AM, Weingartner R, Winder M (2017) Towards mountains without permanent snow and ice. Earth's Future 5:418–435. https://doi.org/10.1002/2016EF000514

Jacobsen D, Milner AM, Brown LE, Dangles O (2012) Biodiversity under threat in glacier-fed river systems. Nat Clim Chang 2:361–364. https://doi.org/10.1038/nclimate1435

Jiménez PA, Dudhia J, González-Rouco JF, Navarro J, Montávez JP, García- Bustamante E (2012) A revised scheme for the WRF surface layer formulation. Mon Weather Rev 140: 898-918. https://doi.org/10.1175/MWR-D-11-00056.1

Junquas C, Takahashi K, Condom T, Espinoza JC, Chavez S, Sicart JE, Lebel T (2018) Understanding the influence of orography on the precipitation diurnal cycle and the associated atmospheric processes in the central Andes. Clim Dyn 50:3995–4017. https://doi.org/10.1007/s00382-017-3858-8

Knutti R, Masson D, Gettelman A (2013) Climate model genealogy: generation CMIP5 and how we got there. Geophys Res Lett 40:1194–1199. https://doi.org/10.1002/grl.50256

Letcher TW, Minder JR (2017) The simulated response of diurnal mountain winds to regionally enhanced warming caused by the snow albedo feedback. J Atmos Sci 74:49–67. https://doi.org/10.1175/JAS-D-16-0158.1

Martinez JA, Arias PA, Castro C, Chang HI, Ochoa-Moya CA (2019) Sea surface temperature-related response of precipitation in northern South America according to a WRF multi-decadal simulation. Int J Climatol 39:2136–2155. https://doi.org/10.1002/joc.5940

Martinez-Castro D, Kumar S, Flores Rojas JL, Moya-Alvarez A, Valdivia Prado JM, Villalobos-Puma E, Del Castillo-Velarde C, Silva-Vidal Y (2019) The impact of microphysics parameterization in the simulation of two convective rainfall events over the central Andes of Peru using WRF-ARW. Atmosphere 10:442. https://doi.org/10.3390/atmos10080442

McGlone D, Vuille M (2012) The associations between El Niño - Southern Oscillation and tropical South American climate in a regional climate model. J Geophys Res 117:D06105. https://doi.org/10.1029/2011JD017066

Meyer JDD, Jin J (2016) Bias correction of the CCSM4 for improved regional climate modeling of the North American monsoon. Clim Dyn 46:2961–2976. https://doi.org/10.1007/s00382-015-2744-5

Michelutti N, Wolfe AP, Cooke CA, Hobbs WA, Vuille M, Smol JP (2015) Climate change forces new ecological states in tropical Andean lakes. PLoS One 10(2):e0115338. https://doi.org/10.1371/journal.pone.0115338

Minder JR, Letcher TW, Liu C (2018) The character and causes of elevation-dependent warming in high-resolution simulations of Rocky Mountain climate change. J Clim 31:2093–2113. https://doi.org/10.1175/JCLI-D-17-0321.1

Mlawer EJ, Taubman SJ, Brown PD, Iacono MJ, Clough SA (1997) Radiative transfer for inhomogeneous atmospheres: RRTM, a validated correlated-k model for the longwave. J Geophys Res 102(D14):16663–16682. https://doi.org/10.1029/97JD00237

Monaghan AJ, Steinhoff DF, Bruyere CL, Yates D (2014) NCAR CESM global bias-corrected CMIP5 output to support WRF/MPAS research. Research data archive at the National Center for Atmospheric Research, Computational and Information Systems Laboratory, Boulder CO. https://doi.org/10.5065/D6DJ5CN4

Mora DE, Willems P (2012) Decadal oscillations in rainfall and air temperature in the Paute River basin – southern Andes of Ecuador. Theor Appl Climatol 108:267–282. https://doi.org/10.1007/s00704-011-0527-4

Morán-Tejeda E, Bazo J, López-Moreno JI, Aguilar E, Azorín-Molina C, Sanchez-Lorenzo A, Martínez R, Nieto JJ, Mejía R, Martín-Hernández N, Vicente-Serrano SM (2016) Climate trends and variability in Ecuador (1966–2011). Int J Climatol 36:3839–3855. https://doi.org/10.1002/joc.4597

Morueta-Holme N, Engemann K, Sandoval-Acuña P, Jonas JD, Segnitz RM, Svenning JC (2015) Strong plant upslope shifts since Humboldt. Proc Natl Acad Sci 112(41):12741–12745. https://doi.org/10.1073/pnas.1509938112

Mourre L, Condom T, Junquas C, Lebel T, Sicart JE, Figueroa R, Cochachin A (2016) Spatio-temporal assessment of WRF, TRMM and in situ precipitation data in a tropical mountain environment (Cordillera Blanca, Peru). Hydrol Earth Syst Sci 20:125–141. https://doi.org/10.5194/hess-20-125-2016

Moya-Alvarez AS, Martinez-Castro D, Flores JL, Silva Y (2018) Sensitivity study on the influence of parameterization schemes in WRF_ARW model on short- and medium-range precipitation forecasts in the Central Andes of Peru. Adv Meteorol 1381092:1–16. https://doi.org/10.1155/2018/1381092

Moya-Alvarez AS, Martinez-Castro D, Kumar S, Estevam R, Silva Y (2019) Response of the WRF model to different resolutions in the rainfall forecast over the complex Peruvian orography. Theor Appl Climatol 137:2993–3007. https://doi.org/10.1007/s00704-019-02782-3

Neale R, Gettelman A, Park S et al (2012) Description of the NCAR Community Atmosphere Model (CAM 5.0). NCAR Technical Note NCAR/TN-486+STR, National Center for Atmospheric Research, 289 pp. http://www.cesm.ucar.edu/models/cesm1. 0/cam/docs/description/cam5_desc.pdf.

Norris J, Carvalho LMV, Jones C, Cannon F et al (2019) Deciphering the contrasting climatic trends between the central Himalaya and Karakoram with 36 years of WRF simulations. Clim Dyn 52:159–180. https://doi.org/10.1007/s00382-018-4133-3

Ochoa A, Campozano L, Sánchez E, Gualán R, Samaniego E (2016) Evaluation of downscaled estimates of monthly temperature and

precipitation for a southern Ecuador case study. Int J Climatol 36: 1244–1255. https://doi.org/10.1002/joc.4418

Pepin N, Bradley R, Diaz H et al (2015) Elevation-dependent warming in mountain regions of the world. Nat Clim Chang 5:424–230. https://doi.org/10.1038/nclimate2563

Posada-Marin JA, Rendón AM, Salazar JF, Mejía JF, Villegas JC (2019) WRF downscaling improves ERA-Interim representation of precipitation around a tropical Andean valley during El Niño: implications for GCM-scale simulation of precipitation over complex terrain. Clim Dyn 52:3609–3629. https://doi.org/10.1007/s00382-018-4403-0

Quishpe-Vásquez C, Gámiz-Fortis SR, García-Valdecasas-Ojeda M, Castro-Díez Y, Esteban-Parra MJ (2019) Tropical Pacific sea surface temperature influence on seasonal streamflow variability in Ecuador. Int J Climatol 39:3895–3914. https://doi.org/10.1002/joc.6047

Rabatel A, Francou B, Soruco A, Gomez J, Cáceres B, Ceballos JL, Basantes R, Vuille M, Sicart JE, Huggel C, Scheel M, Lejeune Y, Arnaud Y, Collet M, Condom T, Consoli G, Favier V, Jomelli V, Galarraga R, Ginot P, Maisincho L, Mendoza J, Ménégoz M, Ramirez E, Ribstein P, Suarez W, Villacis M, Wagnon P (2013) Current state of glaciers in the tropical Andes: a multi-century perspective on glacier evolution and climate change. Cryosphere 7:81–102. https://doi.org/10.5194/tc-7-81-2013

Rasmussen R, Liu C, Ikeda K, Gochis D, Yates D, Chen F, Tewari M, Barlage M, Dudhia J, Yu W, Miller K, Arsenault K, Grubišić V, Thompson G, Gutmann E (2011) High-resolution coupled climate runoff simulations of seasonal snowfall over Colorado: a process study of current and warmer climate. J Clim 24(12):3015–3048. https://doi.org/10.1175/2010JCLI3985.1

Rasmussen R, Ikeda K, Liu C, Gochis D, Clark M (2014) Climate change impacts on the water balance of the Colorado headwaters: high-resolution regional climate model simulations. J Hydrometeorol 15(3):1091–1116. https://doi.org/10.1175/JHM-D-13-0118.1

Recalde-Coronel GC, Barnston AG, Muñoz AG (2014) Predictability of December–April rainfall in Coastal and Andean Ecuador. J Appl Meteorol Climatol 53:1471–1493. https://doi.org/10.1175/JAMC-D-13-0133.1

Rivera JA, Marianetti G, Hinrichs S (2018) Validation of CHIRPS precipitation dataset along the Central Andes of Argentina. Atmos Res 213:437–449. https://doi.org/10.1016/j.atmosres.2018.06.023

Saavedra M, Junquas C, Espinoza JC, Silva Y (2020) Impacts of topography and land use changes on the air surface temperature and precipitation over the central Peruvian Andes. Atmos Res 234:104711. https://doi.org/10.1016/j.atmosres.2019.104711

Saha S, Moorthi S, Pan H et al (2010a) NCEP Climate Forecast System Reanalysis (CFSR) 6-hourly Products, January 1979 to December 2010. Research Data Archive at the National Center for Atmospheric Research, Computational and Information Systems Laboratory, Boulder, CO. https://doi.org/10.5065/D69K487J

Saha S, Moorthi S, Pan HL, Wu X, Wang J, Nadiga S, Tripp P, Kistler R, Woollen J, Behringer D, Liu H, Stokes D, Grumbine R, Gayno G, Wang J, Hou YT, Chuang HY, Juang HMH, Sela J, Iredell M, Treadon R, Kleist D, van Delst P, Keyser D, Derber J, Ek M, Meng J, Wei H, Yang R, Lord S, van den Dool H, Kumar A, Wang W, Long C, Chelliah M, Xue Y, Huang B, Schemm JK, Ebisuzaki W, Lin R, Xie P, Chen M, Zhou S, Higgins W, Zou CZ, Liu Q, Chen Y, Han Y, Cucurull L, Reynolds RW, Rutledge G, Goldberg M (2010b) The NCEP Climate Forecast System Reanalysis. Bull. Amer Meteor Soc 91:1015–1057. https://doi.org/10.1175/2010BAMS3001.1

Segura H, Junquas C, Espinoza JC, Vuille M, Jauregui YR, Rabatel A, Condom T, Lebel T (2019) New insights into the rainfall variability in the tropical Andes on seasonal and interannual time scales. Clim Dyn 53:405–426. https://doi.org/10.1007/s00382-018-4590-8

Segura H, Espinoza JC, Junquas C, Lebel T, Vuille M, Garreaud R (2020) Recent changes in the precipitation-driving processes over the southern tropical Andes/western Amazon. Clim Dyn 54:2613–2631. https://doi.org/10.1007/s00382-020-05132-6

Silva VBS, Kousky VE, Higgins RW (2011) Daily precipitation statistics for South America: an intercomparison between NCEP reanalyses and observations. J Hydrometeorol 12:101–117. https://doi.org/10.1175/2010JHM1303.1

Skamarock W, Klemp JB, Dudhia J, Gill DO, Barker D, Duda MG, Huang X, Wang W (2008) A description of the advanced research WRF version 3. NCAR Technical Note NCAR/TN-475+STR, National Center for Atmospheric Research:113 pp. https://doi.org/10.5065/D68S4MVH/

Solman SA, Blázquez J (2019) Multiscale precipitation variability over South America: analysis of the added value of CORDEX RCM simulations. Clim Dyn 53:1547–1565. https://doi.org/10.1007/s00382-019-04689-1

Taylor K, Stouffer R, Meehl G (2012) An overview of CMIP5 and the experiment design. Bull Amer Meteor Soc 93:485–498. https://doi.org/10.1175/BAMS-D-11-00094.1

Tewari M, Chen F, Wang W et al (2004) Implementation and verification of the unified Noah land surface model in the WRF model. 20th Conference on Weather Analysis and Forecasting/16th Conference on Numerical Weather Prediction, Seattle, WA, Amer Meteor Soc, 14.2A. https://ams.confex.com/ams/pdfpapers/69061.pdf

Thompson DW, Barnes EA, Deser C, Foust WE, Phillips AS (2015) Quantifying the role of internal climate variability in future climate trends. J Clim 28:6443–6456. https://doi.org/10.1175/JCLI-D-14-00830.1

Tiedtke M (1989) A comprehensive mass flux scheme for cumulus parameterization in large-scale models. Mon Weather Rev 117(8): 1779–1800. https://doi.org/10.1175/1520-0493(1989)117%3C1779:ACMFSF%3E2.0.CO;2

Tobar V, Wyseure G (2018) Seasonal rainfall patterns classification, relationship to ENSO and rainfall trends in Ecuador. Int J Climatol 38: 1808–1819. https://doi.org/10.1002/joc.5297

Toride K, Iseri Y, Duren A, England JF, Kavvas ML (2019) Evaluation of physical parameterizations for atmospheric river induced precipitation and application to long-term reconstruction based on three reanalysis datasets in Western Oregon. Sci Total Environ 658:570–581. https://doi.org/10.1016/j.scitotenv.2018.12.214

Urrutia R, Vuille M (2009) Climate Change projections for the tropical Andes using a regional climate model: temperature and precipitation simulations for the end of the 21st century. J Geophys Res 114: D02108. https://doi.org/10.1029/2008JD011021

van Vuuren DP, Edmonds J, Kainuma M, Riahi K, Thomson A, Hibbard K, Hurtt GC, Kram T, Krey V, Lamarque JF, Masui T, Meinshausen M, Nakicenovic N, Smith SJ, Rose SK (2011) The representative concentration pathways: an overview. Clim Chang 109:5–31. https://doi.org/10.1007/s10584-011-0148-z

Vicente-Serrano SM, Aguilar E, Martinez R et al (2017) The complex influence of ENSO on droughts in Ecuador. Clim Dyn 48:405–427. https://doi.org/10.1007/s00382-016-3082-y

Viviroli D, Archer D, Buytaert W et al (2011) Climate Change and mountain water resources: overview and recommendations for research, management and policy. Hydrol Earth Syst Sci 15:471–504. https://doi.org/10.5194/hess-15-471-2011

Vuille M, Bradley RS (2000) Mean annual temperature trends and their vertical structure in the tropical Andes. Geophys Res Lett 27:3885–3888. https://doi.org/10.1029/2000GL011871

Vuille M, Bradley RS, Keimig F (2000) Climate variability in the Andes of Ecuador and its relation to tropical Pacific and Atlantic sea surface temperature anomalies. J Clim 13:2520–2535. https://doi.org/10.1175/1520-0442(2000)013<2520:CVITAO>2.0.CO;2

Vuille M, Bradley RS, Werner M, Keimig F (2003) 20th century climate change in the tropical Andes: observations and model results. Clim Chang 59(1-2):75–99. https://doi.org/10.1023/A:1024406427519

Vuille M (2013) Climate change and water resources in the tropical Andes. Interamerican Development Bank Technical Note No. IDB-TN-515. https://publications.iadb.org/publications/english/document/Climate-Change-and-Water-Resources-in-the-Tropical-Andes.pdf

Vuille M, Franquist E, Garreaud R, Lavado W, Caceres B (2015) Impact of the global warming hiatus on Andean temperature. J Geophys Res 120(9):3745–3757. https://doi.org/10.1002/2015JD02312

Vuille M, Carey M, Huggel C, Buytaert W, Rabatel A, Jacobsen D, Soruco A, Villacis M, Yarleque C, Elison Timm O, Condom T, Salzmann N, Sicart JE (2018) Rapid decline of snow and ice in the tropical Andes – impacts, uncertainties and challenges ahead. Earth Sci Rev 176:195–213. https://doi.org/10.1016/j.earscirev.2017.09.019

Wang W, Bruyère C, Duda et al (2016) ARW version 3 modeling system user's guide. NCAR. http://www2.mmm.ucar.edu/wrf/users/docs/user_guide_ V3.7/ARWUsersGuideV3.7.pdf

Zhang C, Wang Y, Hamilton K (2011) Improved representation of boundary layer clouds over the southeast Pacific in ARW-WRF using a modified Tiedtke cumulus parameterization scheme. Mon Weather Rev 139(11):3489–3513. https://doi.org/10.1175/MWR-D-10-05091.1